Enhanced methanol production via selective hydrogen utilization during CO_2 hydrogenation over Co containing dual-atom doped oxide catalyst

*Nazmul Hasan MD Dostagir,[a] Carlo Robert Tomuschat,[a,b] Atsushi Fukuoka,[a] and Abhijit Shrotri[a]**

[a] Institute for Catalysis, Hokkaido University, Kita 21 Nishi 10, Kita-ku, Sapporo, Hokkaido 001-0021, Japan

[b] Department of Chemistry, TUM School of Natural Sciences, Technical University of Munich, Lichtenbergstraße 4, 85748 Garching, Germany

* Email: ashrotri@cat.hokudai.ac.jp, fukuoka@cat.hokudai.ac.jp

Abstract

Capturing hydrogen with CO_2 to produce methanol is becoming increasingly intriguing. Renewable H_2 is expensive and is currently produced in a limited amount. Therefore, selective utilization of H_2 towards methanol formation, which has been paid little attention to, is necessary without being wasted towards side product formation. Here, we show that using Co containing dual-atom doped oxide (Co-Zn-ZrO_2) catalyst H_2 utilization can be selectively directed towards methanol formation and at the same time, H_2 wastage can be minimized by suppressing competitive CO formation. Co-Zn-ZrO_2 produced methanol with space time yield of 1.5 g_{MeOH} h^{-1} g_{cat}^{-1}, which is one of the highest ever reported under industrially relevant conditions. In this catalyst, Co was responsible for CO_2 activation and formate stabilization and made Zn free of formate poisoning, which helped in easy H_2 dissociation promoting formate hydrogenation to methanol. When Co was replaced with other metals (for example: Pd, Ni and Cu), H_2 utilization was promoted more towards CO formation than

towards methanol formation decreasing methanol selectivity. This work represents the potential of Co containing dual-atom doped oxide catalyst for selectively utilizing H_2 for methanol formation while identifying the underlying factor for controlling H_2 utilization towards methanol or CO formation.

KEYWORD: CO_2 hydrogenation to methanol, selective H_2 utilization, selectivity control, formate pathway, doped oxide

Introduction

Hydrogen plays important roles in the energy sector and chemical synthesis despite not being an energy resource. It is almost not available naturally on earth and currently is mainly produced from non-renewable fossil fuels leading to an increase in CO_2 emission.[1] Renewable H_2 (for example: formed via water electrolysis, biomass reforming using renewable energy sources) is more expensive than non-renewable H_2.[2,3] Therefore, H_2 needs to be stored and transported efficiently and safely. In this regard, methanol received much attention as a hydrogen carrier.[4,5] H_2 is stored as methanol in a liquid form via CO_2 hydrogenation reaction ($CO_2 + 3\ H_2 \leftrightarrow CH_3OH + H_2O$) and methanol can also be reacted to give the H_2 back forming a closed cycle. Therefore, during methanol formation via CO_2 hydrogenation reaction, hydrogen should be efficiently used for methanol production without being wasted for the formation of side products. Although CO_2 hydrogenation to methanol is a heavily investigated reaction, little attention has been paid to the selective utilization of hydrogen towards methanol formation.

One of the main problems in the way of utilizing H_2 efficiently towards methanol formation is the consumption of H_2 towards other side products mainly CO via reverse water-gas shift (RWGS) reaction ($CO_2 + H_2 \leftrightarrow CO + H_2O$).[4] Therefore, obtaining methanol with high productivity and selectivity and suppressing side product formation at the same time are

highly important in order to selectively utilize H_2 for methanol formation. In this regard, oxides like In_2O_3, doped oxides (for example: M_aO_x-ZrO_2; M_a = Zn, Cd, Ga) are important candidates as catalysts for CO_2 hydrogenation to methanol reaction.[6,7,8–11] They showed good selectivity of methanol albeit with poor methanol productivity because of their poor H_2 dissociation ability. Metal promoters were added to promote methanol productivity.[12,13,22–27,14–21] However, methanol selectivity decreased although methanol productivity increased.[14,15,17,18,22,26–30]

Oxygen vacancies present on the surface of the oxide catalysts act as the active site for CO_2 activation, H_2 activation and formate intermediate stabilization.[31] However, strong adsorption of CO_2 and formate poison the active site by blocking it for H_2 dissociation leading to poor utilization of H_2 towards methanol production.[32–35] Consequently, methanol selectivity and productivity decreased and selectivity of CO increased.[36–38] Addition of metal promoters promotes H_2 dissociation ability.[12,13,22–27,14–21] These extra dissociated hydrogen species are not controllable to be selectively utilized for methanol synthesis. Instead, they are used up for promoting RWGS reaction more than methanol formation.[14,15,17,18,22,26–30] Thus, methanol selectivity decreased. Therefore, using a metal promoter for hydrogen dissociation is not a helpful way to utilize H_2 selectively for methanol formation.

In literature, little information is available on controlling H_2 consumption towards methanol formation selectively. Heterolytic dissociation of H_2 has been suggested as the promotional factor for methanol formation.[39] However, promotion of RWGS reaction despite heterolytic H_2 dissociation by promoter has also been suggested.[14,40] Due to inability to detect the underlying factor for controlling H_2 utilization towards methanol formation, development of efficient catalyst capable of selectively utilizing H_2 for methanol formation becomes difficult.

Herein, we show that instead of directly promoting H_2 dissociation by adding metal promoters, creating a site that are responsible for CO_2 adsorption and formate intermediate stabilization and are different from that for H_2 dissociation can selectively utilize H_2 towards methanol formation and suppress H_2 wastage via side product formation. We have previously shown that the introduction of Co single atom in oxide structure creates oxygen deficient interfacial active sites for CO_2 adsorption and is helpful to mitigate the poisoning effect of CO_2 and formate on the H_2 dissociation element.[41,42] In this piece of work, we prepared Co, Zn doped ZrO_2 (Co-Zn-ZrO_2) dual-atom doped oxide catalyst. We found that as compared to Zn-ZrO_2, Co-Zn-ZrO_2 increased H_2 consumption for methanol formation and suppressed H_2 consumption for RWGS reaction at the same time promoting both methanol selectivity and productivity. Co-Zn-ZrO_2 produced methanol with space time yield (STY_{MeOH}) of 1.5 g_{MeOH} h^{-1} g_{cat}^{-1} under industrially relevant conditions, which is one of the highest STY_{MeOH} ever reported. Detailed analysis showed that in Co-Zn-ZrO_2, Co atoms created separate active sites and controlled CO_2 adsorption and formate stabilization and Zn sites being free of formate poisoning easily dissociated H_2 to hydrogenate the formate adsorbed on Co-Zr interfacial site selectively to methanol. At the same time, CO formation via formate decomposition was also suppressed. When Co was changed to other metals (for example: Cu, Pd and Ni), they promoted H_2 dissociation and created sites for side reaction wasting H_2 through RWGS reaction. As a result, methanol selectivity decreased. We found that the intrinsic activity of metal promoters for CO_2 hydrogenation is inversely proportional to the methanol selectivity in the dual-atom oxides. This work shows that catalysts designed based on the preferential adsorption of CO_2 and H_2 lead to the maximum use of H_2 for methanol formation and minimize H_2 wastage through side reactions.

Results and Discussion

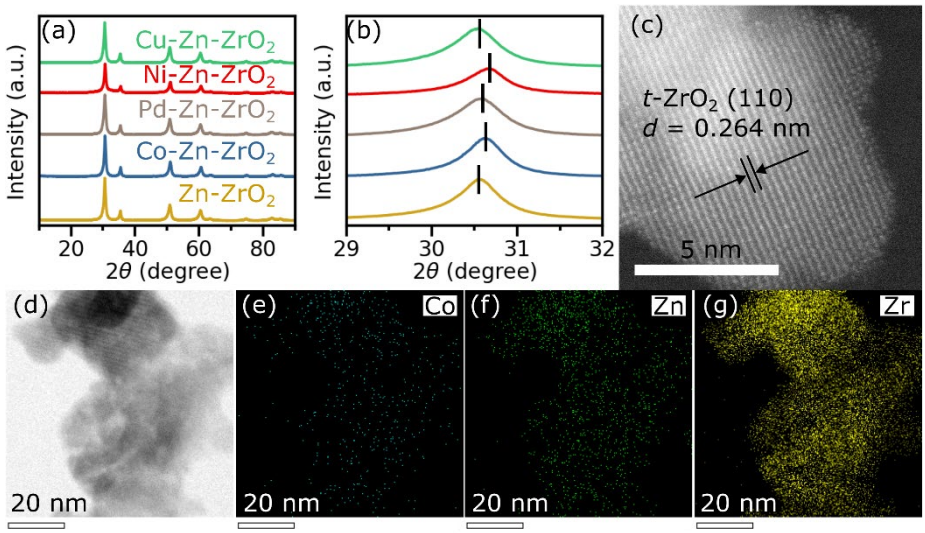

Figure 1: (a) XRD of all dual-atom doped oxides and Zn-ZrO_2 with (b) the shift of the (101) reflection of *t*-ZrO_2. (c) HAADF-STEM image of Co-Zn-ZrO_2 showing the (110) plane of *t*-ZrO_2 and the corresponding d spacing. (d) HAADF-STEM image of Co-Zn-ZrO_2 with elemental mapping of (e) Co, (f) Zn and (g) Zr.

All catalysts with ZrO_2 as the bulk phase were prepared by coprecipitation of metal salts in ammonia solution followed by washing, drying and then calcination at 500 °C under air (see supporting information for detailed procedure). All doped oxide catalysts showed tetragonal ZrO_2 structure as observed in the X-ray diffraction (XRD) pattern (Figure 1a). No feature for individual oxide of dopants was observed. With increase in dopant concentration (shown in Figure S1), the 2θ value corresponding to the (101) plane of *t*-ZrO_2 shifted to higher value as compared to that of Zn-ZrO_2 (Figure 1b) because dopants have smaller ionic radii than that of Zr^{4+} ($r_{Zr^{4+}}$ = 0.84 Å).[43] In the high angle annular dark-field scanning transmission electron microscopy (HAADF-STEM) image of Co-Zn-ZrO_2, only *t*-ZrO_2 phase was visible. (Figure 1c). Elemental mapping using energy dispersive X-ray (EDX) analysis (Figure 1d-g) showed homogeneous distribution of Co and Zn atoms.

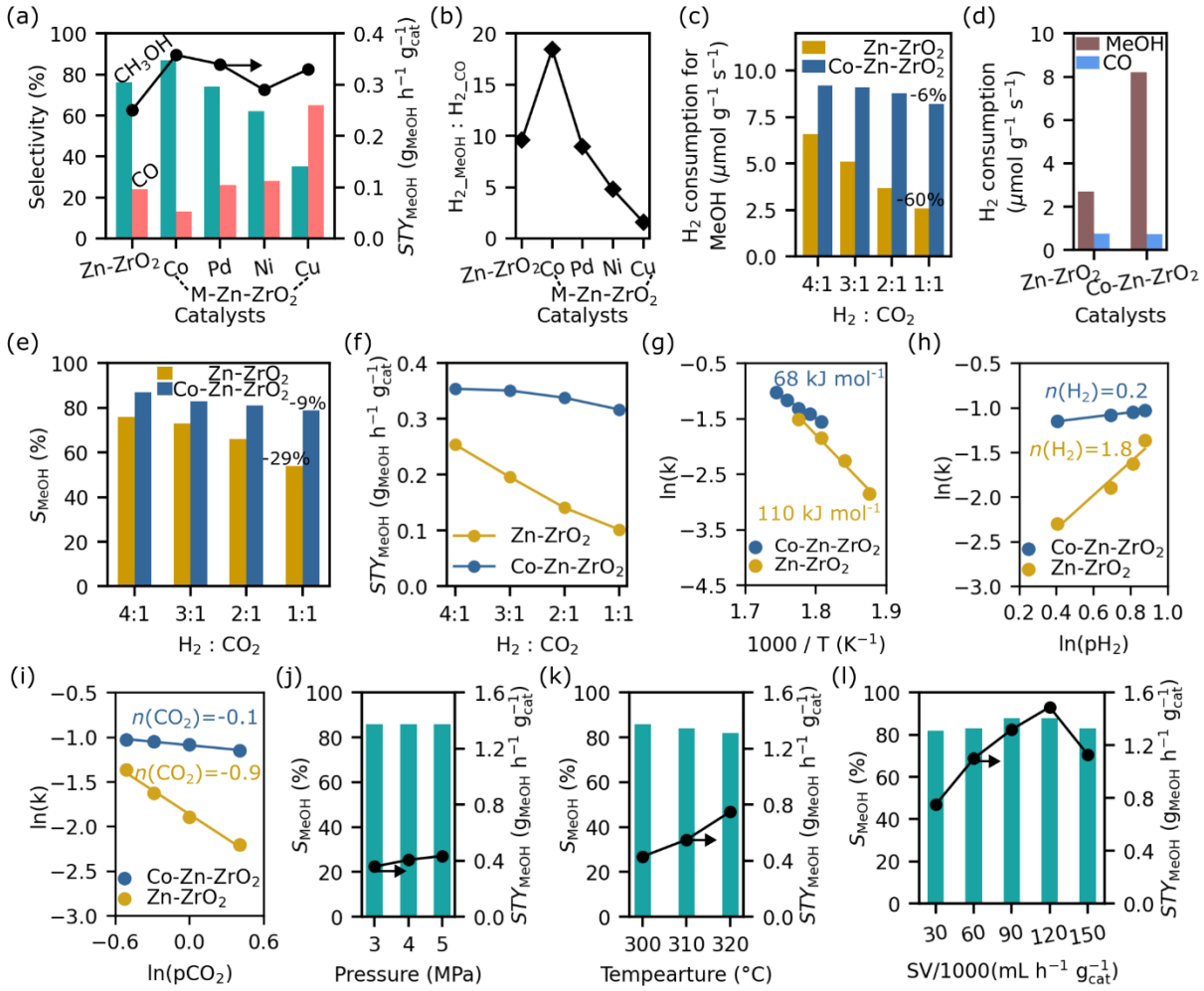

Figure 2: (a) Comparison of catalytic activity between Zn-ZrO_2 and Co-Zn-ZrO_2. (b) Ratio of H_2 consumption between methanol and CO over different catalysts. (c) H_2 consumption towards methanol synthesis under variable H_2:CO_2 ratio. (d) H_2 consumption towards methanol and CO synthesis at H_2/CO_2 = 1. (e) Comparison of methanol selectivity over Zn-ZrO_2 and Co-Zn-ZrO_2 under variable H_2:CO_2 ratio. (f) Methanol productivity over Zn-ZrO_2 and Co-Zn-ZrO_2 under variable H_2:CO_2 ratio. (g) Activation energy of methanol formation over Zn-ZrO_2 and Co-Zn-ZrO_2. Order of methanol formation with respect to (h) H_2 (n_{H_2}) and (i) CO2 (n_{CO_2}). Rate of products were taken in mol g_{cat}^{-1} h^{-1}. Effect of pressure (j), temperature at 5 MPa (k) and space velocity at 320 °C and 5 MPa (l) on methanol selectivity and productivity. Reaction condition: 300 °C, 3 MPa, 30,000 mL h^{-1} g_{cat}^{-1}, H_2/CO_2 = 4 unless otherwise mentioned.

The performance of all catalysts in CO_2 hydrogenation reaction was evaluated in a stainless-steel fixed bed flow reactor (Figure S1). Undoped ZrO_2 showed (Table S2) negligible CO_2 conversion indicating that dopants were solely responsible for catalytic activity. First of all, we compared the catalytic activity of single atom doped Zn-ZrO_2 and dual atom doped *M*-Zn-ZrO_2 (M = Co, Pd, Ni and Cu) catalysts at 300 °C, 3 MPa, 30000 mL h^{-1} g_{cat}^{-1}, H_2:CO_2 = 4:1 (Figure 2a and Table S2). Methanol selectivity (S_{MeOH}) and

productivity over Zn-ZrO_2 were 76% and 0.25 g_{MeOH} h^{-1} g_{cat}^{-1} respectively. When a third element was introduced, STY_{MeOH} increased. However, S_{MeOH} increased only when Co was introduced. In the case of Co-Zn-ZrO_2, S_{MeOH} increased to 87% and methanol productivity increased to 0.36 g_{MeOH} h^{-1} g_{cat}^{-1}. The S_{MeOH} and STY_{MeOH} of Co-Zn-ZrO_2 were much higher than that over single-atom analogues (Zn-ZrO_2 and Co-ZrO_2) and their physical mixture (Zn-ZrO_2 + Co-ZrO_2) (Figure S2a). Among them, Co-Zn-ZrO_2 showed the lowest space time yield of CO (STY_{CO}) (Figure S2b). Therefore, presence of Co in dual-atom doped oxide selectively promotes methanol formation while suppressed CO formation at the same time. All other dual atom *M*-Zn-ZrO_2 (M = Pd, Ni and Cu) oxide catalysts showed lower S_{MeOH} than Zn-ZrO_2. Along with the decrease in S_{MeOH}, introduction of Pd, Ni and Cu increased both STY_{CO} and S_{CO} (Table S2 and figure S3). These results are in line with reported literature.[14,15,17,18,22,26,27] The effect of Co to increase both S_{MeOH} and STY_{MeOH} was further confirmed by carrying out reaction in a wide temperature range (260 – 360 °C) (Figure S4). At 260 °C, methanol selectivity over Zn-ZrO_2 was 80%, which was increased to 98% over Co-Zn-ZrO_2. The latter showed higher S_{MeOH} and STY_{MeOH} than Zn-ZrO_2 even at unfavorable temperature range for methanol synthesis (> 300 °C).

Next, to understand the usage of H_2 towards methanol and CO formation over different catalysts, we calculated the ratio between H_2 utilization towards methanol to that towards CO formation (H_2 (MeOH) : H_2 (CO)) (Figure 2b). For Zn-ZrO_2, the H_2 (MeOH) : H_2 (CO) ratio was 9.6. For Co-Zn-ZrO_2, the ratio increased to 18. Whereas, for other catalysts the ratio decreased as compared to that of Zn-ZrO_2. The ratio decreased the most for Cu-Zn-ZrO_2. This result shows that over Co-Zn-ZrO_2, H_2 was used selectively for methanol formation and H_2 wastage towards CO was suppressed. On the other hand, presence of Pd, Ni and Cu, although increased methanol productivity, increased wastage of H_2 to a much higher degree due to promotion of CO formation. To understand the consumption of H_2 over Co-Zn-

ZrO_2 in more detail, we compared the H_2 consumption over Co-Zn-ZrO_2 and Zn-ZrO_2 under varying H_2:CO_2 ratio (Figure 2c). When H_2:CO_2 ratio was changed from 4:1 to 1:1, the H_2 consumption towards methanol synthesis decreased by 6% over Co-Zn-ZrO_2. In comparison, over Zn-ZrO_2, H_2 consumption towards methanol synthesis decreased by 60%. At H_2:CO_2 ratio of 1:1, while the H_2 consumption towards CO formation was similar, H_2 consumption towards methanol formation for Co-Zn-ZrO_2 was 3 times higher than that for Zn-ZrO_2 (Figure 2d). As a result of the better H_2 utilization towards methanol formation over Co-Zn-ZrO_2 as compared to Zn-ZrO_2, the former showed much higher S_{MeOH} (Figure 2e) and STY_{MeOH} (Figure 2f) as compared to the latter even in H_2 lean conditions ($H_2/CO_2 < 3$, less than the stoichiometric requirement). To better understand the ability of Co-Zn-ZrO_2 to produce methanol selectively even under low H_2 partial pressure, we calculated the activation energy (E_a) for methanol formation over Co-Zn-ZrO_2 and Zn-ZrO_2 (Figure 2g). E_a for methanol formation over Zn-ZrO_2 was 110 kJ mol^{-1}. Over Co-Zn-ZrO_2, it was reduced to 68 kJ mol^{-1}. For Zn-ZrO_2, the order of methanol formation with respect to H_2 (n_{H_2}) was 1.8 (Figure 2h) and that with respect to CO_2 (n_{CO_2}) was –0.9 (Figure 2i). In comparison, over the Co-Zn-ZrO_2 catalyst the n_{H_2} and n_{CO_2} were 0.25 and –0.13, respectively. Higher negative value of n_{CO_2} for Zn-ZrO_2 indicates that adsorption of CO_2 on the active site of Zn-ZrO_2 inhibited methanol formation. These results are in line with reported literature[44] and it has been shown that methanol selectivity reduces over oxide catalysts because the adsorption of intermediates and H_2 dissociation occur on the same site.[36,38] Higher positive value of n_{H_2} for Zn-ZrO_2 indicates that higher partial pressure of H_2 is needed for methanol formation. On the contrary, over Co-Zn-ZrO_2, values of n_{H_2} and n_{CO_2} close to zero suggest less dependency on both H_2 and CO_2 partial pressure. These different n_{H_2} and n_{CO_2} over Co-Zn-ZrO_2 indicate that the sites for CO_2 activation and H_2 dissociation are different in Co-Zn-ZrO_2.[42]

After confirming the directional property of Co in H_2 utilization towards methanol synthesis, catalytic performance of Co-Zn-ZrO_2 were optimized by varying reaction parameters. Increasing pressure has a positive effect on methanol productivity (Figure 2j). With increasing pressure from 3 MPa to 5 MPa at 300 °C and 30,000 mL h^{-1} g_{cat}^{-1}, STY_{MeOH} increased from 0.36 g_{MeOH} h^{-1} g_{cat}^{-1} to 0.43 g_{MeOH} h^{-1} g_{cat}^{-1}. Increasing reaction temperature from 300 °C to 320 °C at 5 MPa increased STY_{MeOH} from 0.43 g_{MeOH} h^{-1} g_{cat}^{-1} to 0.75 g_{MeOH} h^{-1} g_{cat}^{-1} (Figure 2k). S_{MeOH} remained similar. Changing space velocity had a positive effect on both S_{MeOH} and STY_{MeOH} until 120,000 mL h^{-1} g_{cat}^{-1}, beyond which both decreased (Figure 2l). Increasing space velocity from 30,000 mL h^{-1} g_{cat}^{-1} to 120,000 mL h^{-1} g_{cat}^{-1} at 5 MPa and 320 °C increased STY_{MeOH} from 0.75 g_{MeOH} h^{-1} g_{cat}^{-1} to 1.5 g_{MeOH} h^{-1} g_{cat}^{-1}, which is one of the highest STY_{MeOH} reported so far under industrially relevant conditions (Table S3). The Co-Zn-ZrO_2 catalysts showed robustness against change in reaction conditions and showed stability during a 100 h long catalytic test (Figure S5a). XRD analysis of the used catalyst after 100 h showed no change (Figure S5b) and XPS analysis confirmed that Co^{2+}, Zn^{2+} and Zr^{4+} did not change oxidation state after the reaction (Figure S5c-e). Elemental mapping analysis confirmed no agglomeration of Co or Zn species showing high dispersion (Figure S5f-i).

H_2 dissociation ability

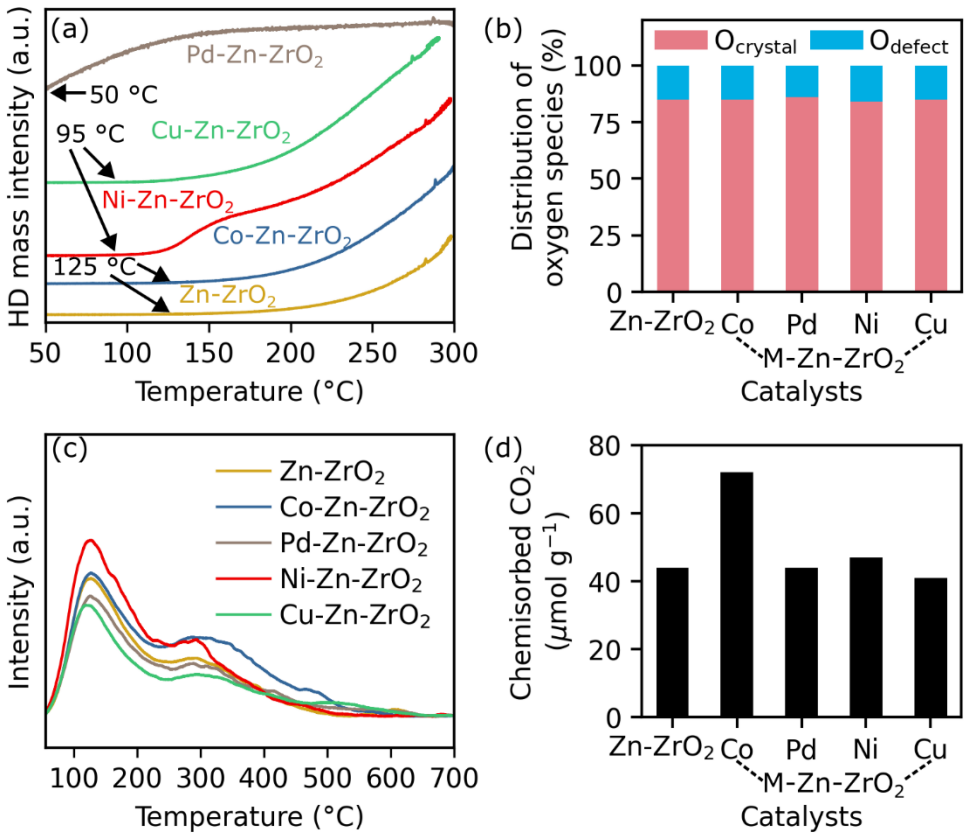

Figure 3: (a) Mass intensity of HD in H_2-D_2 isotope exchange experiment over all catalysts. (b) Relative oxygen defect content calculated from O 1S XPS, (c) CO_2 TPD spectra and (d) amount of CO_2 chemisorbed over all the dual-atom doped oxides in comparison to Zn-ZrO_2.

There are two direct ways to influence methanol selectivity and productivity. One is to influence H_2 dissociation while the other is to influence CO_2 adsorption and formate intermediate stabilization. Therefore, first we checked whether Co increased the H_2 dissociation ability to improve H_2 utilization towards methanol synthesis. To do so, we compared the ability of HD formation of all catalysts in H_2-D_2 isotope exchange experiment (Figure 3a). In this experiment, H_2 and D_2 dissociated over the surface of catalysts and formed HD. If HD formation starts at lower temperature over one catalyst, it indicates that the catalyst has high H_2 dissociation ability as compared to other catalysts. The onset temperature for HD formation over Zn-ZrO_2 was around 125 °C, which was similar to that

over Co-Zn-ZrO_2. As compared to Zn-ZrO_2 and Co-Zn-ZrO_2, the onset temperature for HD formation was lower over Cu-Zn-ZrO_2 (95 °C), Ni-Zn-ZrO_2 (95 °C) and Pd-Zn-ZrO_2 (50 °C). This indicates that the introduction of Co did not increase the H_2 dissociation ability. Unlike Co, introduction of Pd, Ni and Cu increased H_2 dissociation ability. The ability of Co to utilize H_2 selectively for methanol synthesis despite its inability to promote H_2 dissociation as compared to other metals indicates that Co must take part directly in CO_2 adsorption and formate intermediate stabilization and influences H_2 dissociation and its utilization indirectly.

CO_2 activation ability

To understand the CO_2 activation ability, first we analyzed the presence of oxygen vacancy over different catalysts because oxygen vacancy present on the oxide surface serves as the active site for CO_2 activation.[41] The density of defective oxygen species was measured by the O 1s XPS analysis (Figure S6). The relative amount of O_{defect} was 16% for Zn-ZrO_2 (Figure 3b). Incorporation of a dopant (Co, Pd, Ni, Cu) did not increase the O_{defect}. Next, in the CO_2 temperature programmed desorption (CO_2 TPD) analysis of pre-adsorbed CO_2, two desorption features were observed (Figure 4c). The low temperature feature (100-250 °C) indicates the desorption of physisorbed and weakly adsorbed CO_2 species whereas the high temperature feature (250-500 °C) indicates the desorption of chemisorbed CO_2 species, which is the main reactive species for methanol formation. Among all the catalysts, Co-Zn-ZrO_2 increased CO_2 chemisorption (72 µmol g^{-1}) as compared to Zn-ZrO_2 (44 µmol g^{-1}) (Figure 4d). In comparison, Pd-Zn-ZrO_2, Ni-Zn-ZrO_2 and Cu-Zn-ZrO_2 showed similar CO_2 chemisorption (41, 47 and 44 µmol g^{-1}) to Zn-ZrO_2. For Co-Zn-ZrO_2, increased CO_2 chemisorption despite having similar density of oxygen defect to Zn-ZrO_2 indicates that Co changes the chemical environment around the oxygen vacancy so that the CO_2 is strongly chemisorbed. This is in line with our previous report where introduction of Co^{2+} single atom in ZrO_2 created oxygen vacancy around Co atoms, which were responsible for CO_2

chemisorption at Co-V_o-Zr (V_o = oxygen vacancy) interfacial site.[41] Therefore, presence of Co in the dual-atom doped oxide structure controls CO_2 activation.

Site for formate adsorption

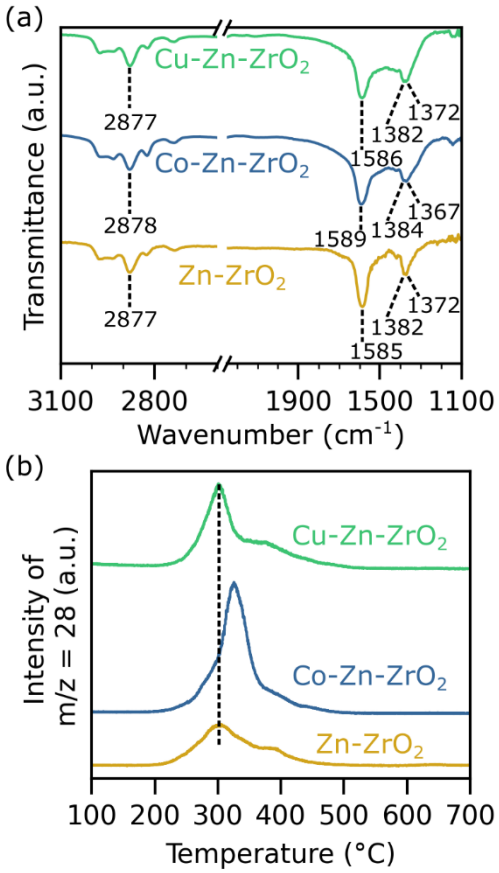

Figure 4: (a) Comparison of IR peak positions of formate species stabilized over Zn-ZrO_2, Co-Zn-ZrO_2 and Cu-Zn-ZrO_2 under steady state during in situ DRIFTS experiment (reaction condition: 300 °C, 0.1 MPa, H_2/CO_2 = 4). (b) Mass intensity of m/z = 28 during HCOOH TPD experiments over the three doped catalysts.

Over oxide catalysts, formate is the key intermediate for CO_2 hydrogenation to methanol as well as CO.[7,36,41,45] In order to understand the formate stabilization site over different catalysts, in situ diffuse reflectance infrared Fourier transform spectroscopy (DRIFTS) analysis was carried out at 300 °C, 0.1 MPa, H_2:CO_2 = 4 (Figure S7). Bidentate

formate bonded with two Zr atoms is the most stable formate configuration in undoped ZrO_2.[10,46,47] In comparison to undoped ZrO_2, formate peak positions were shifted in the presence of doped oxides (Figure S8). This indicates that in the doped oxides formate is stabilized at M-Zr (M = dopant) interface. We compared Zn-ZrO_2, Co-Zn-ZrO_2 and Cu-Zn-ZrO_2 (Cu-Zn-ZrO_2 being the most CO selective was chosen among the other three dual-atom doped oxides) (Figure 4a). The formate peak positions over Co-Zn-ZrO_2 were similar to Co-ZrO_2 and shifted from that over Zn-ZrO_2 (Figure S8 and 5a). This indicates that the formate stabilization site over Co-Zn-ZrO_2 was Co-Zr interfacial site (Figure S9). This was in line with reported literature that Co-Zr interface stabilizes formate species.[41,42] When Co was changed to Cu, formate peak positions over Cu-Zn-ZrO_2 were similar to that over Zn-ZrO_2. This indicates that over Cu-Zn-ZrO_2, formate stabilization site was Zn-Zr interface, similar to Zn-ZrO_2.

For further confirmation, we performed temperature programmed decomposition of adsorbed formic acid (HCOOH TPD) over catalysts surface (Figure 4b). Decomposition of adsorbed formic acid over Co-Zn-ZrO_2 resulted in CO formation with a peak centered at 340 °C while the decomposition profile for both Zn-ZrO_2 and Cu-Zn-ZrO_2 showed CO formation at lower temperature (300 °C). These results confirm that Co site in Co-Zn-ZrO_2 was responsible for CO_2 adsorption and stabilization of formate. Over Co-Zn-ZrO_2, formate became more stabilized as compared to that over Zn-ZrO_2 and Cu-Zn-ZrO_2. Better stabilization of formate might be the reason behind suppression of CO formation via formate decomposition. On the other hand, when Cu was used, it did not take part in formate stabilization. Therefore, promotion of RWGS reaction over Cu-Zn-ZrO_2 may be a result of excessive CO_2 hydrogenation to CO over Cu site itself.

Selective utilization of H_2 towards methanol formation: Co-Zn cooperation

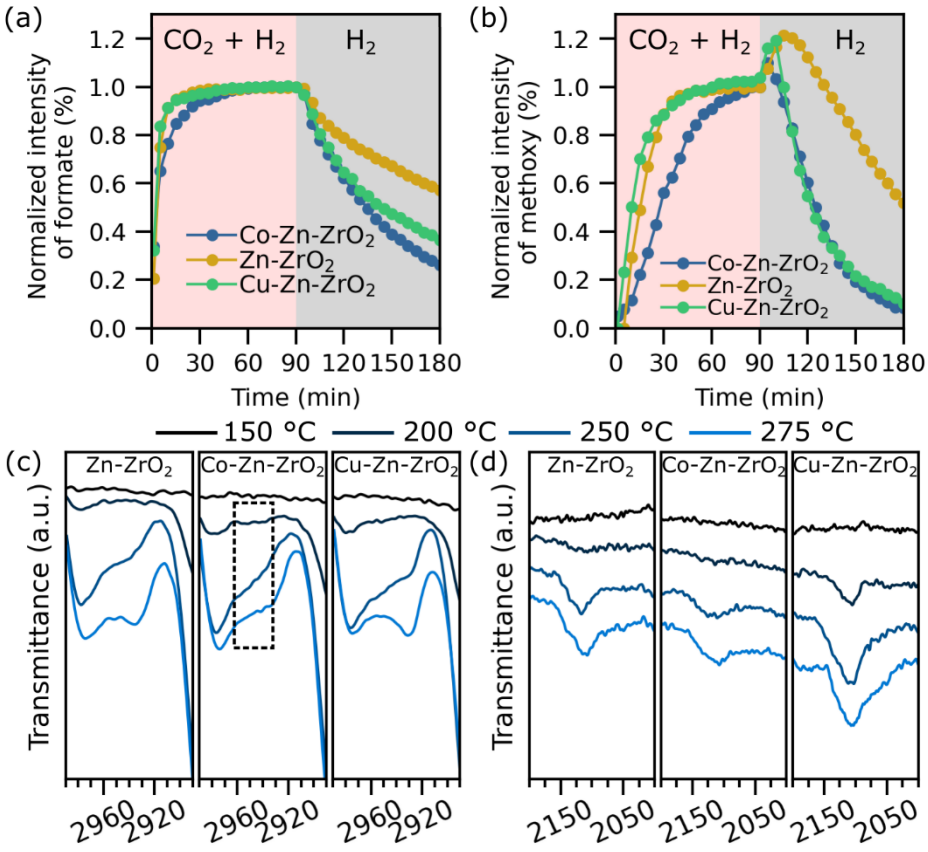

Figure 5: Normalized intensity of (a) formate and (b) methoxy species during in situ DRIFTS analysis of Zn-ZrO_2, Co-Zn-ZrO_2 and Cu-Zn-ZrO_2. Reaction condition: 300 °C, 0.1 MPa, H_2 : CO_2 = 4. In situ DRIFTS analysis for the production of (c) methoxy and (d) CO under different temperatures. Reaction condition: T °C, 0.1 MPa, H_2 : CO_2 = 4.

To realize the selective utilization of H_2 towards methanol formation resulting enhanced methanol selectivity and productivity, we studied in situ DRIFTS analysis. For methanol formation over oxide surface, the reaction pathway follows successive hydrogenation of formate to methoxy species adsorbed on the surface followed by desorption of methoxy as methanol.[45] Time resolved evolution of adsorbed species was measured by in situ DRIFTS under CO_2 hydrogenation condition (Figure 5a, b). Complete DRIFTS spectra for all catalysts and detailed peak assignment are shown in Figure S10-S12 and Table S4. At the start of the reaction, formate species appeared rapidly along with carbonate over all doped catalysts

indicating formate formation was easy over all three catalysts. Methoxy species first appeared on the surface of Co-Zn-ZrO_2 followed by Cu-Zn-ZrO_2 and Zn-ZrO_2 indicating the high activity of Co-Zn-ZrO_2 towards methanol synthesis. After formate and methoxy reached the steady state under CO_2 and H_2 atmosphere, CO_2 flow was stopped to monitor the consumption of formate and methoxy species. Formate was consumed faster over Co-Zn-ZrO_2 than over Zn-ZrO_2. The rate of disappearance of methoxy over Co-Zn-ZrO_2 was also faster than that over Zn-ZrO_2. These results indicate that, formate adsorbed over the Co-Zr interface was more reactive. In addition, the desorption of methoxy species adsorbed over Co-Zn-ZrO_2 surface was also facile. Slow consumption of formate over Zn-ZrO_2 indicates that H_2 dissociation over Zn atoms in presence of formate is difficult. Moreover, methoxy was not observed in Co-ZrO_2 catalyst during in situ DRIFTS analysis (Figure S13) indicating that only Co single atom cannot dissociate H_2 in presence of formate. Therefore, it is evident that in Co-Zn-ZrO_2, hydrogen was dissociated over Zn atoms to promote the hydrogenation of formate species adsorbed on Co-Zr interface to produce methanol. It is worth mentioning that in Co-Zn-ZrO_2, Zn being free of CO_2 and formate (as Co controls CO_2 activation and formate stabilization) dissociates H_2 easily promoting formate hydrogenation to methanol. This cooperative effect was further confirmed by temperature dependent in-situ DRIFTS study (Figure 5c, d). Peak for adsorbed methoxy species appeared at a lower temperature over Co-Zn-ZrO_2 than over Zn-ZrO_2. On the other hand, Co-Zn-ZrO_2 produced CO formation at higher temperature as compared to Zn-ZrO_2 and showed much lower CO formation than Zn-ZrO_2. Hence, it is evident that dissociated hydrogen species over Zn sites were mainly consumed for methoxy formation and H_2 wastage via RWGS reaction was also suppressed.

When Co was replaced to Cu, the rate of consumptions for formate and methoxy species over Cu-Zn-ZrO_2 were in between that over Co-Zn-ZrO_2 and Zn-ZrO_2, which is in line with the STY_{MeOH} exerted by them (Figure 5a, b). In the temperature dependent in situ DRIFTS

study (Figure 5c), methoxy formation over Cu-Zn-ZrO_2 started at higher temperature as compared to Co-Zn-ZrO_2. Rather Cu-Zn-ZrO_2 started CO formation at much lower temperature (Figure 5d). CO peak intensity for Cu-Zn-ZrO_2 was much more intense than that over Zn-ZrO_2 and Co-Zn-ZrO_2. Considering the same formate stabilization site for both Zn-ZrO_2 and Cu-Zn-ZrO_2 (as shown by HCOOH TPD experiment), slower formate consumption rate for Cu-Zn-ZrO_2 than that Co-Zn-ZrO_2 (in line with STY_{MeOH}) and high H_2 dissociating ability for Cu-Zn-ZrO_2 (as shown in the study of H_2 dissociation ability), it can be said that Cu itself creates a new active site for the promotion of RWGS in Cu-Zn-ZrO_2 catalyst. In literature it has also been reported that dopant single atom can create its own CO_2 hydrogenation site to promote side reaction in methanol synthesis.[40] Therefore, in order to effectively utilizing H_2 for methanol formation, use of Co to create CO_2 activation and formation stabilization site is more important than the use of a metal promoter (for example Cu, Ni, Pd) that promotes H_2 dissociation.

Mechanism

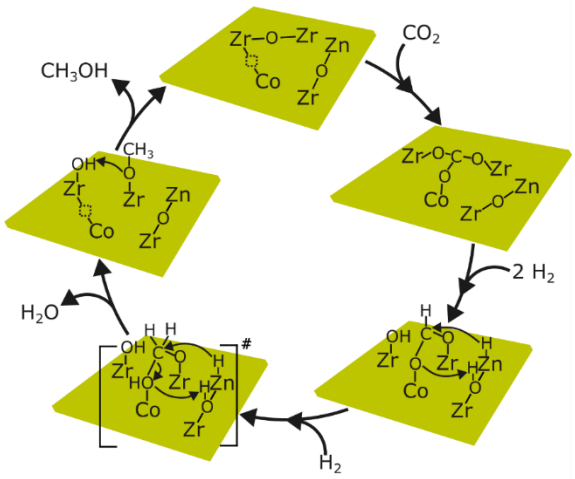

Figure 6: Mechanism of methanol formation over Co-Zn-ZrO_2 catalyst.

Based on the above results we propose the following mechanism for CO_2 hydrogenation to methanol over Co-Zn-ZrO_2 catalyst through cooperative effect of the Co and Zn (Figure 6).

Doping of Co^{2+} generates creates oxygen vacant site for adsorption of CO_2. First H_2 dissociation might happen on either Co or Zn atoms for hydrogenation of adsorbed CO_2, although the presence of Zn promotes hydrogenation of adsorbed CO_2 to formate. Following formate formation, the ability of Co to dissociate H_2 and hydrogenate formate is hindered. Instead, H_2 dissociated over adjacent Zn atoms facilitates hydrogenation of formate to methoxy species and promotes the desorption of methoxy species as methanol. Because the stability of formate is increased and formate gets selectively hydrogenated to methoxy by the cooperation of Co and Zn atoms, the chance of CO formation via formate decomposition was low. Furthermore, because Co controls CO_2 adsorption, the possibility of CO formation over Zn site also became low due to lack of available CO_2. Thus, the presence of Co on one hand promoted methanol formation and on the other hand suppressed CO formation. As a result, hydrogen dissociated over Zn atoms was selectively utilized for methanol formation. Consequently, both the S_{MeOH} and STY_{MeOH} were increased. Being free of poisonous effect of CO_2 and formate, Zn atoms assisted in H_2 dissociation and hydrogenation of adsorbed intermediates to methanol more freely. Consequently, higher S_{MeOH} can be obtained even at low H_2 partial pressure. Thus, the introduction of Co in the oxide structure directed the utilization of H_2 selectively towards methanol formation. If Co was changed to another metal (Pd, Ni, Cu), which can only promote H_2 dissociation ability, the chance of side product formation over that metal increased due to intrinsic CO_2 hydrogenation ability of that metal.

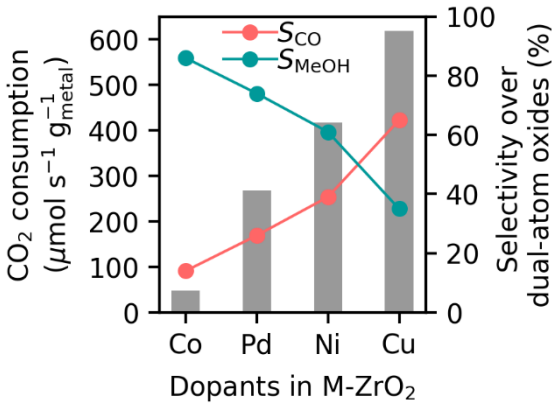

Figure 7: Correlation between specific CO_2 consumption activity of metal dopants and product selectivity over dual-atom doped oxide catalysts.

To test this theory, we calculated intrinsic CO_2 consumption rate for Co, Pd, Ni and Cu and related it with the S_{MeOH} and S_{CO} of the corresponding dual-atom doped oxides. For calculating intrinsic CO_2 consumption rate over a metal, we calculated the dopant metal specific CO_2 consumption rate of the corresponding single-atom doped oxide. Because undoped ZrO_2 is inactive in CO_2 hydrogenation, the activity of single-atom doped oxides can be attributed to the intrinsic activity of the corresponding doped metals. Figure 7 shows the result. Among Co, Ni, Pd and Cu, Co has the lowest intrinsic activity in CO_2 consumption and the corresponding Co-Zn-ZrO_2 showed the highest S_{MeOH} and the lowest S_{CO}. With increasing the specific activity of metals, the S_{MeOH} of the corresponding dual-atom doped oxide decreased. Therefore, to effectively steer H_2 utilization towards methanol synthesis, focusing on intermediate stabilization and their effective conversion to methanol is more important than focusing on uncontrollable promotion in H_2 dissociation. The latter would rather waste H_2 by utilizing it towards CO formation and would decrease S_{MeOH}.

Discussion

In order to effectively capture and store H_2 as methanol, oxide catalysts are important as they produce methanol with good selectivity although H_2 utilization remained poor due to low methanol productivity because of poor H_2 dissociation ability. Metal promoters were used to

promote H_2 dissociation, but they promote competing RWGS reaction more than methanol formation. Herein, we prepared Co-Zn-ZrO_2 dual-atom doped oxide which selectively promoted H_2 utilization for methanol formation and at the same time suppressed H_2 utilization for CO formation thus, promoting both methanol selectivity and productivity. Detailed analysis found that introduction of Co controls CO_2 adsorption and formate stabilization by creating oxygen vacant sites near itself. Thus, Zn became free of CO_2 and formate poisoning and dissociated H_2 easily and promoted formate hydrogenation to methanol. When other metals having high H_2 dissociation ability (for example: Pd, Cu, Ni) were used instead of Co, they promoted H_2 dissociation and promoted RWGS more than methanol formation. As a result, although methanol productivity increased, methanol selectivity decreased. This study showed that tuning of CO_2 and formate adsorption site is a better approach than promoting H_2 dissociation in order to selectively promote H_2 utilization for methanol synthesis. We belief that this work will inspire to take into account the efficient utilization of H_2 in hydrogenation reactions.

Supporting Information

Acknowledgement

This work was supported by JSPS Grant-in-Aid for Scientific Research (C) KAKENHI JP22K04821 and research fund from The Japan Petroleum Institute. This work was also supported by Iketani Science and Technology Foundation. A part of this work was supported by “Advanced Research Infrastructure for Materials and Nanotechnology in Japan (ARIM)” of the Ministry of Education, Culture, Sports, Science and Technology (MEXT). Grant Number JPMXP122HK0089 (Hokkaido University).

References

(1) Lubitz, W.; Tumas, W. Hydrogen: An Overview. *Chem. Rev.* **2007**, *107*, 3900–3903.

(2) Hassan, Q.; Abdulateef, A. M.; Hafedh, S. A.; Al-samari, A.; Abdulateef, J.; Sameen, A. Z.; Salman, H. M.; Al-Jiboory, A. K.; Wieteska, S.; Jaszczur, M. Renewable Energy-to-Green Hydrogen: A Review of Main Resources Routes, Processes and Evaluation. *Int. J. Hydrogen Energy*. **2023**, *48*, 17383–17408.

(3) Turner, J.; Sverdrup, G.; Mann, M. K.; Maness, P. C.; Kroposki, B.; Ghirardi, M.; Evans, R. J.; Blake, D. Renewable Hydrogen Production. *Int. J. Energy Res.* **2008**, *32* (5), 379–407.

(4) Frei, M. S.; Mondelli, C.; Short, M. I. M.; Pérez-Ramírez, J. Methanol as a Hydrogen Carrier: Kinetic and Thermodynamic Drivers for Its CO_2-Based Synthesis and Reforming over Heterogeneous Catalysts. *ChemSusChem* **2020**, *13* (23), 6330–6337.

(5) Niermann, M.; Drünert, S.; Kaltschmitt, M.; Bonhoff, K. Liquid Organic Hydrogen Carriers (LOHCs)-Techno-Economic Analysis of LOHCs in a Defined Process Chain. *Energy Environ. Sci.* **2019**, *12* (1), 290–307.

(6) Martin, O.; Martín, A. J.; Mondelli, C.; Mitchell, S.; Segawa, T. F.; Hauert, R.; Drouilly, C.; Curulla-Ferré, D.; Pérez-Ramírez, J. Indium Oxide as a Superior Catalyst for Methanol Synthesis by CO_2 Hydrogenation. *Angew. Chemie - Int. Ed.* **2016**, *55* (21), 6261–6265.

(7) Wang, J.; Zhang, G.; Zhu, J.; Zhang, X.; Ding, F.; Zhang, A.; Guo, X.; Song, C. CO_2 Hydrogenation to Methanol over In_2O_3-Based Catalysts: From Mechanism to Catalyst Development. *ACS Catal.* **2021**, *11* (3), 1406–1423.

(8) Feng, W. H.; Yu, M. M.; Wang, L. J.; Miao, Y. T.; Shakouri, M.; Ran, J.; Hu, Y.; Li, Z.; Huang, R.; Lu, Y. L.; Gao, D.; Wu, J. F. Insights into Bimetallic Oxide Synergy

during Carbon Dioxide Hydrogenation to Methanol and Dimethyl Ether over $GaZrO_x$ Oxide Catalysts. *ACS Catal.* **2021**, *11* (8), 4704–4711.

(9) Tada, S.; Ochiai, N.; Kinoshita, H.; Yoshida, M.; Shimada, N.; Joutsuka, T.; Nishijima, M.; Honma, T.; Yamauchi, N.; Kobayashi, Y.; Iyoki, K. Active Sites on $Zn_xZr_{1-X}O_{2-x}$ Solid Solution Catalysts for CO_2-to-Methanol Hydrogenation. *ACS Catal.* **2022**, *12*, 7748–7759.

(10) Wang, J.; Li, G.; Li, Z.; Tang, C.; Feng, Z.; An, H.; Liu, H.; Liu, T.; Li, C. A Highly Selective and Stable ZnO-ZrO_2 Solid Solution Catalyst for CO_2 Hydrogenation to Methanol. *Sci. Adv.* **2017**, *3* (10).

(11) Wang, J.; Tang, C.; Li, G.; Han, Z.; Li, Z.; Liu, H.; Cheng, F.; Li, C. High-Performance $MaZrO_x$ (Ma = Cd, Ga) Solid-Solution Catalysts for CO_2 Hydrogenation to Methanol. *ACS Catal.* **2019**, *9* (11), 10253–10259.

(12) Frei, M. S.; Mondelli, C.; García-Muelas, R.; Kley, K. S.; Puértolas, B.; López, N.; Safonova, O. V.; Stewart, J. A.; Curulla Ferré, D.; Pérez-Ramírez, J. Atomic-Scale Engineering of Indium Oxide Promotion by Palladium for Methanol Production via CO_2 Hydrogenation. *Nat. Commun.* **2019**, *10* (1), 1–11.

(13) Pinheiro Araújo, T.; Mondelli, C.; Agrachev, M.; Zou, T.; Willi, P. O.; Engel, K. M.; Grass, R. N.; Stark, W. J.; Safonova, O. V.; Jeschke, G.; Mitchell, S.; Pérez-Ramírez, J. Flame-Made Ternary Pd-In_2O_3-ZrO_2 Catalyst with Enhanced Oxygen Vacancy Generation for CO_2 Hydrogenation to Methanol. *Nat. Commun.* **2022**, *13* (1), 1–12.

(14) Lee, K.; Anjum, U.; Araújo, T. P.; Mondelli, C.; He, Q.; Furukawa, S.; Pérez-Ramírez, J.; Kozlov, S. M.; Yan, N. Atomic Pd-Promoted $ZnZrO_x$ Solid Solution Catalyst for CO_2 Hydrogenation to Methanol. *Appl. Catal. B Environ.* **2022**, *304*, 120994.

(15) Lee, K.; Mendes, P. C. D.; Jeon, H.; Song, Y.; Dickieson, M. P.; Anjum, U.; Chen, L.; Yang, T. C.; Yang, C. M.; Choi, M.; Kozlov, S. M.; Yan, N. Engineering Nanoscale H Supply Chain to Accelerate Methanol Synthesis on $ZnZrO_x$. *Nat. Commun.* **2023**, *14* (1), 819.

(16) Sun, K.; Rui, N.; Zhang, Z.; Sun, Z.; Ge, Q.; Liu, C. J. A Highly Active Pt/In_2O_3 catalyst for CO_2 hydrogenation to Methanol with Enhanced Stability. *Green Chem.* **2020**, *22* (15), 5059–5066.

(17) Xu, D.; Hong, X.; Liu, G. Highly Dispersed Metal Doping to ZnZr Oxide Catalyst for CO_2 Hydrogenation to Methanol: Insight into Hydrogen Spillover. *J. Catal.* **2021**, *393*, 207–214.

(18) Dostagir, N. H. M.; Thompson, C.; Kobayashi, H.; Karim, A. M.; Fukuoka, A.; Shrotri, A. Rh Promoted In_2O_3 as a Highly Active Catalyst for CO_2 Hydrogenation to Methanol. *Catal. Sci. Technol.* **2020**, *10* (24), 8196–8202.

(19) Li, M. M.; Zou, H.; Zheng, J.; Wu, T.; Chan, T.; Soo, Y.; Wu, X.; Gong, X.; Chen, T.; Roy, K.; Held, G.; Tsang, S. C. E. Methanol Synthesis at a Wide Range of H_2/CO_2 Ratios over a Rh-In Bimetallic Catalyst. *Angew. Chemie* **2020**, *132* (37), 16173–16180.

(20) Rui, N.; Wang, X.; Deng, K.; Moncada, J.; Rosales, R.; Zhang, F.; Xu, W.; Waluyo, I.; Hunt, A.; Stavitski, E.; Senanayake, S. D.; Liu, P.; Rodriguez, J. A. Atomic Structural Origin of the High Methanol Selectivity over In_2O_3-Metal Interfaces: Metal-Support Interactions and the Formation of a InO_x Overlayer in Ru/In_2O_3 Catalysts during CO_2 Hydrogenation. *ACS Catal.* **2023**, *13*, 3187–3200.

(21) Shen, C.; Sun, K.; Zou, R.; Wu, Q.; Mei, D.; Liu, C. J. CO_2 Hydrogenation to Methanol on Indium Oxide-Supported Rhenium Catalysts: The Effects of Size. *ACS Catal.* **2022**, *12* (20), 12658–12669.

(22) Frei, M. S.; Mondelli, C.; García-Muelas, R.; Morales-Vidal, J.; Philipp, M.; Safonova, O. V.; López, N.; Stewart, J. A.; Ferré, D. C.; Pérez-Ramírez, J. Nanostructure of Nickel-Promoted Indium Oxide Catalysts Drives Selectivity in CO_2 Hydrogenation. *Nat. Commun.* **2021**, *12* (1), 1–9.

(23) Song, L.; Wang, H.; Wang, S.; Qu, Z. Dual-Site Activation of H_2 over $Cu/ZnAl_2O_4$ Boosting CO_2 Hydrogenation to Methanol. *Appl. Catal. B Environ.* **2023**, *322*, 122137.

(24) Bavykina, A.; Yarulina, I.; Al Abdulghani, A. J.; Gevers, L.; Hedhili, M. N.; Miao, X.; Galilea, A. R.; Pustovarenko, A.; Dikhtiarenko, A.; Cadiau, A.; Aguilar-Tapia, A.; Hazemann, J.-L.; Kozlov, S. M.; Oud-Chikh, S.; Cavallo, L.; Gascon, J. Turning a Methanation Co Catalyst into an In–Co Methanol Producer. *ACS Catal.* **2019**, *9* (8), 6910–6918.

(25) Li, L.; Yang, B.; Gao, B.; Wang, Y.; Zhang, L.; Ishihara, T.; Qi, W.; Guo, L. CO_2 Hydrogenation Selectivity Shift over In-Co Binary Oxides Catalysts: Catalytic Mechanism and Structure-Property Relationship. *Chinese J. Catal.* **2022**, *43* (3), 862–876.

(26) Zhu, J.; Cannizzaro, F.; Liu, L.; Zhang, H.; Kosinov, N.; Filot, I. A. W.; Rabeah, J.; Brückner, A.; Hensen, E. J. M. Ni-In Synergy in CO_2 Hydrogenation to Methanol. *ACS Catal.* **2021**, *11* (18), 11371–11384.

(27) Han, X.; Xiao, T.; Li, M.; Hao, Z.; Chen, J.; Pan, Y.; Zi, X.; Zhang, H.; Xi, S.; Wai, H. M.; Kawi, S.; Ma, X. Synergetic Interaction between Single-Atom Cu and Ga_2O_3 Enhances CO_2 Hydrogenation to Methanol over $CuGaZrO_x$. *ACS Catal.* **2023**, *13* (20), 13679–13690.

(28) Jia, X.; Sun, K.; Wang, J.; Shen, C.; Liu, C. jun. Selective Hydrogenation of CO_2 to Methanol over Ni/In_2O_3 Catalyst. *J. Energy Chem.* **2020**, *50*, 409–415.

(29) Wang, J.; Sun, K.; Jia, X.; Liu, C. jun. CO_2 Hydrogenation to Methanol over Rh/In_2O_3 Catalyst. *Catal. Today* **2021**, *365*, 341–347.

(30) Rui, N.; Wang, Z.; Sun, K.; Ye, J.; Ge, Q.; Liu, C. jun. CO_2 Hydrogenation to Methanol over Pd/In_2O_3: Effects of Pd and Oxygen Vacancy. *Appl. Catal. B Environ.* **2017**, *218*, 488–497.

(31) Ye, J.; Liu, C.; Mei, D.; Ge, Q. Active Oxygen Vacancy Site for Methanol Synthesis from CO_2 Hydrogenation on In_2O_3 (110): A DFT Study. *ACS Catal.* **2013**, *3* (6), 1296–1306.

(32) Kattel, S.; Yan, B.; Yang, Y.; Chen, J. G.; Liu, P. Optimizing Binding Energies of Key Intermediates for CO_2 Hydrogenation to Methanol over Oxide-Supported Copper. *J. Am. Chem. Soc.* **2016**, *138* (38), 12440–12450.

(33) Jung, K. D.; Bell, A. T. Role of Hydrogen Spillover in Methanol Synthesis over Cu/ZrO_2. *J. Catal.* **2000**, *193* (2), 207–223.

(34) Tang, C.; Tang, S.; Sha, F.; Han, Z.; Feng, Z.; Wang, J.; Li, C. Insights into the Selectivity Determinant and Rate-Determining Step of CO_2 Hydrogenation to Methanol. *J. Phys. Chem. C* **2022**, *126* (25), 10399–10407.

(35) Polierer, S.; Jelic, J.; Pitter, S.; Studt, F. On the Reactivity of the Cu/ZrO_2 System for the Hydrogenation of CO_2 to Methanol: A Density Functional Theory Study. *J. Phys. Chem. C* **2019**, *123* (44), 26904–26911.

(36) Chen, T. Y.; Cao, C.; Chen, T. B.; Ding, X.; Huang, H.; Shen, L.; Cao, X.; Zhu, M.; Xu, J.; Gao, J.; Han, Y. F. Unraveling Highly Tunable Selectivity in CO_2 Hydrogenation over Bimetallic In-Zr Oxide Catalysts. *ACS Catal.* **2019**, *9* (9), 8785–8797.

(37) Fang, H.; Zhao, G.; Cheng, D.; Liu, J.; Lan, D.; Jiang, Q.; Liu, X.; Ge, J.; Xu, Z.; Xu, H. MOF-Derived Bimetallic Core–Shell Catalyst HZSM-5@ZrO_2–In_2O_3: High CO_2 Conversion in Reverse Water Gas Shift Reaction. *Mater. Chem. Front.* **2022**.

(38) Šot, P.; Noh, G.; Weber, I. C.; Pratsinis, S. E.; Copéret, C. The Influence of ZnO−ZrO_2 Interface in Hydrogenation of CO_2 to CH_3OH. *Helv. Chim. Acta* **2022**, *105* (3), e202200007.

(39) Han, Z.; Tang, C.; Wang, J.; Li, L.; Li, C. Atomically Dispersed Pt^{n+} Species as Highly Active Sites in Pt/In_2O_3 Catalysts for Methanol Synthesis from CO_2 Hydrogenation. *J. Catal.* **2021**, *394*, 236–244.

(40) Cannizzaro, F.; Hensen, E. J. M.; Filot, I. A. W. The Promoting Role of Ni on In_2O_3 for CO_2 Hydrogenation to Methanol. *ACS Catal.* **2023**, *13*, 1875–1892.

(41) Dostagir, N. H. M.; Rattanawan, R.; Gao, M.; Ota, J.; Hasegawa, J. Y.; Asakura, K.; Fukouka, A.; Shrotri, A. Co Single Atoms in ZrO_2 with Inherent Oxygen Vacancies for Selective Hydrogenation of CO_2 to CO. *ACS Catal.* **2021**, *11* (15), 9450–9461.

(42) Dostagir, N. H. M.; Tomuschat, C. R.; Oshiro, K.; Gao, M.; Hasegawa, J. Y.; Fukuoka, A.; Shrotri, A. Mitigating the Poisoning Effect of Formate during CO_2 Hydrogenation to Methanol over Co-Containing Dual-Atom Oxide Catalysts. *JACS Au* **2024**, *50*, 27.

(43) Shannon, R. D. Revised Effective Ionic Radii and Systematic Studies of Interatomic Distances in Halides and Chalcogenides. *Acta Crystallogr. Sect. A* **1976**, *32* (5), 751–767.

(44) Yang, C.; Pei, C.; Luo, R.; Liu, S.; Wang, Y.; Wang, Z.; Zhao, Z. J.; Gong, J. Strong Electronic Oxide-Support Interaction over In_2O_3/ZrO_2 for Highly Selective CO_2 Hydrogenation to Methanol. *J. Am. Chem. Soc.* **2020**, *142* (46), 19523–19531.

(45) Feng, Z.; Tang, C.; Zhang, P.; Li, K.; Li, G.; Wang, J.; Feng, Z.; Li, C. Asymmetric Sites on the $ZnZrO_x$ Catalyst for Promoting Formate Formation and Transformation in CO_2 Hydrogenation. *J. Am. Chem. Soc.* **2023**.

(46) Pokrovski, K.; Jung, K. T.; Bell, A. T. Investigation of CO and CO_2 Adsorption on Tetragonal and Monoclinic Zirconia. *Langmuir* **2001**, *17* (14), 4297–4303.

(47) Korhonen, S. T.; Calatayud, M.; Outi I Krause, A. Structure and Stability of Formates and Carbonates on Monoclinic Zirconia: A Combined Study by Density Functional Theory and Infrared Spectroscopy. *J. Phys. Chem. C* **2008**, *112* (41), 16096–16102.